

EXPERIMENTAL SLOSHING CHARACTERISTICS AND A MECHANICAL
ANALOGY OF LIQUID SLOSHING IN A SCALE-MODEL
CENTAUR LIQUID OXYGEN TANK

By Irving E. Sumner, Andrew J. Stofan, and Daniel J. Shramo

Lewis Research Center
Cleveland, Ohio

NATIONAL AERONAUTICS AND SPACE ADMINISTRATION

For sale by the Office of Technical Services, Department of Commerce,
Washington, D.C. 20230 -- Price \$0.75

EXPERIMENTAL SLOSHING CHARACTERISTICS AND A MECHANICAL

ANALOGY OF LIQUID SLOSHING IN A SCALE-MODEL

CENTAUR LIQUID OXYGEN TANK

by Irving E. Sumner, Andrew J. Stofan, and Daniel J. Shramo

Lewis Research Center

SUMMARY

An experimental investigation of liquid sloshing in a 1/3.75 scale-model Centaur stage liquid oxygen tank was conducted to determine (1) the fundamental frequencies of oscillation, (2) the horizontal slosh forces and damping ratios (logarithmic decrements) occurring at the fundamental frequencies, and (3) the slosh damping effectiveness of a proposed slosh baffle. Experimental data were obtained for clean, unbaffled, and baffled tank configurations. The measurement of vertical and horizontal slosh forces enabled the determination of quantities for a pendulum analogy that would effectively describe liquid sloshing in the unbaffled tank configuration. Several quantities determined for such an analogy included: (1) the length of the pendulum arm, (2) the maximum angles through which the pendulum can oscillate, (3) the hinge point location of the pendulum, (4) the pendulum or sloshing mass, (5) the fixed or nonsloshing mass, and (6) the geometric centroid location of the fixed mass. The results of this investigation are presented in terms of dimensionless parameters that are applicable to tanks of any size having similar configurations.

INTRODUCTION

Propellant sloshing is a potential source of disturbance critical to the stability of space vehicles that contain relatively large masses of liquid propellants. Oscillations of the propellant masses result from the lateral displacement or angular rotation of the vehicle during the powered phase of the flight. These perturbations of vehicle motion may be caused by wind gusts during boost, rapid changes in vehicle angle of attack, altitude stabilization control pulses, or bending of the vehicle itself. Severe sloshing results when the propellant oscillations are coupled with one or more of the perturbations of vehicle motion at nearly the fundamental or first natural mode frequency of the contained propellant.

A complete dynamic-stability analysis of the vehicle must include the forces produced by the liquid motion in partly filled propellant tanks. Propellant sloshing in a specific tank is generally represented by a mechanical

model (either a pendulum or a spring-mass analogy). The equations of motion of the mechanical model are then included in the equations of motion of the entire vehicle. Several quantities necessary to effectively describe propellant sloshing as a pendulum analogy, for example, are: (1) the length of the pendulum arm, (2) the maximum angles through which the pendulum can oscillate, (3) the hinge point location of the pendulum, (4) the pendulum or sloshing mass, (5) the fixed or nonsloshing mass, and (6) the centroid location of the fixed mass. Many analytical investigations have been made (e.g., refs. 1 to 5) to determine the values of these quantities for several tank configurations over a range of liquid depths. Since the results of these investigations yielded a wide range of values that could be used for several of the previously mentioned quantities for a given tank configuration and liquid depth, the accuracy of the mechanical model was not known.

Preliminary computer studies (using analytical values in the mechanical sloshing model) of the stability of the Atlas-Centaur space vehicle indicated that an instability problem occurred during the booster-powered phase of the flight. The instability of the vehicle was caused by propellant sloshing in the Centaur stage liquid oxygen tank. During the simulated booster-powered phase of the flight, the Centaur liquid oxygen tank was filled to a liquid depth ratio (liquid height/tank height) of approximately 0.80 and contained about 44 cubic feet of ullage.

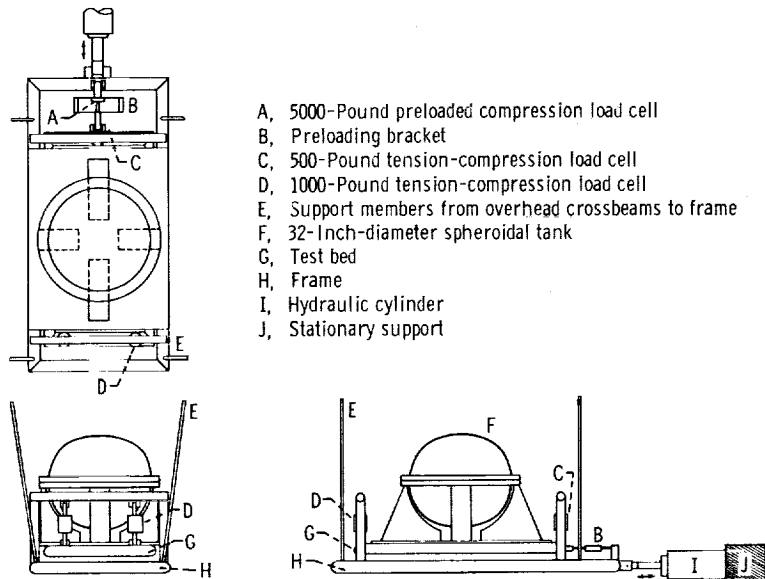
A slosh baffle located at a depth ratio (distance from baffle to bottom of tank/tank height) of about 0.75 was proposed to suppress and damp the propellant oscillations. It was necessary, therefore, to determine the fundamental frequencies of oscillation, the slosh forces, and the damping ratios for the unbaffled and baffled Centaur liquid oxygen tank configurations. The Centaur liquid oxygen tank and proposed slosh baffle differed enough from configurations previously investigated (e.g., refs. 6 to 11) so that the available experimental data could not be applied with confidence. In addition, it was necessary to experimentally determine a suitable mechanical model that would accurately represent the propellant sloshing in the unbaffled Centaur liquid oxygen tank configuration.

An experimental investigation of liquid sloshing in a 1/3.75 scale-model Centaur stage liquid oxygen tank was conducted at the NASA Lewis Research Center to determine (1) the fundamental frequencies of oscillation, (2) the maximum horizontal slosh forces and damping ratios occurring at the fundamental frequencies, and (3) the slosh damping effectiveness of the proposed slosh baffle. Experimental data were obtained over a range of liquid depth ratios for the following tank configurations: (1) clean tank with no internal hardware, (2) unbaffled tank that included simulated internal flight hardware such as the thrust distribution cylinder (or thrust barrel), the spring ring, and the vent and fill pipes, and (3) the baffled tank that included the proposed slosh baffle and supporting structure in addition to the same internal hardware used in the unbaffled tank. The measurement of vertical and horizontal slosh forces enabled the determination of quantities for a pendulum analogy that would effectively describe liquid sloshing in the unbaffled tank configuration. The contained liquid was water in most tests. The results of this investigation are presented in terms of dimensionless parameters.

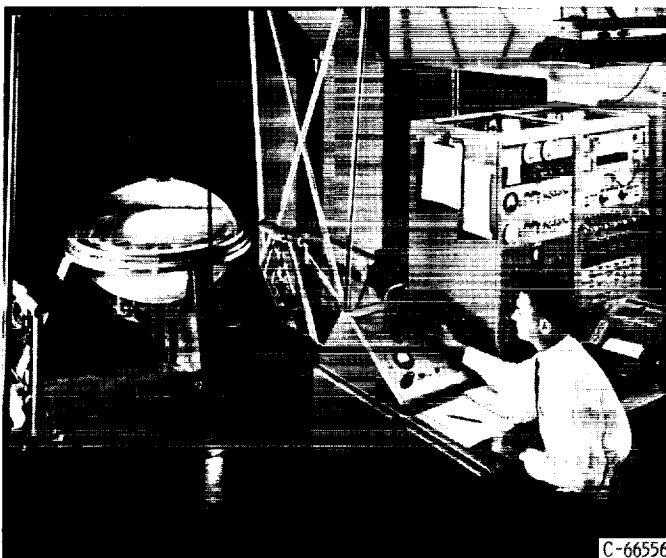
APPARATUS AND INSTRUMENTATION

Test Facility

The experimental test facility, which is nearly identical to that described in reference 10, is shown in figure 1. The scale-model Centaur liquid



(a) Schematic view.



(b) Pictorial view.

Figure 1. - Experimental test facility.

oxygen tank was mounted on a test bed that was suspended from a frame through three vertically oriented load cells and one horizontally oriented load cell. The frame was suspended from overhead crossbeams and was free to oscillate in one direction in the horizontal plane. A hydraulic piston and cylinder provided the driving force. The excitation amplitude could be varied from 0 to 1 inch, and the excitation frequency could be varied from 0 to 20 cycles per second. A sinusoidal excitation waveform was used in this investigation. The electric and hydraulic control circuits for the driving mechanism were designed to enable the oscillatory motion of the frame, the test bed, and the tank to be

"quick-stopped" at a point of zero velocity during any given cycle of oscillation so that only the residual forces resulting from the liquid sloshing could be measured.

The horizontal load cell was a piezoelectric quartz crystal that had been preloaded in compression. The single vertical load cell supporting one end of the test bed was a semiconductor-type transducer, while the other two vertical load cells were strain-gage-type transducers. The quartz crystal and semiconductor load cells were the only ones having sufficient sensitivity and accuracy for this investigation and were, therefore, the only load

cells used to obtain experimental data. The horizontal and vertical slosh forces were displayed on a continuously recording strip chart. The vertical forces occurring at each end of the test bed were assumed to be of equal magnitude but 180° out of phase.

Scale-Model Tank and Internal Hardware

A $1/3.75$ scale model (fig. 2(a)) of the oblate spheroidal Centaur liquid

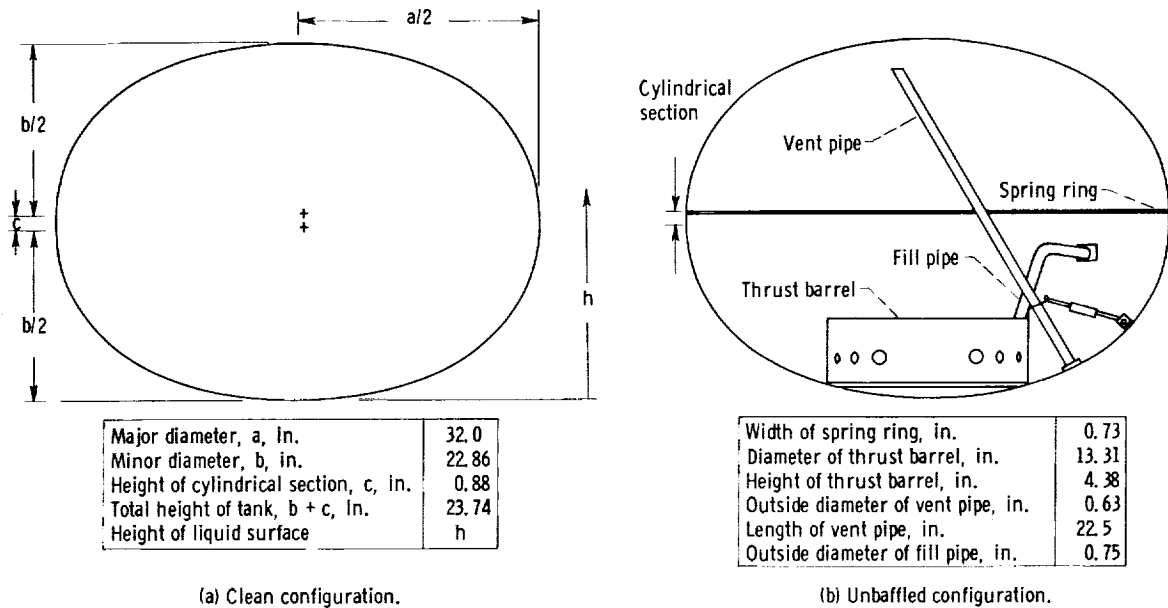
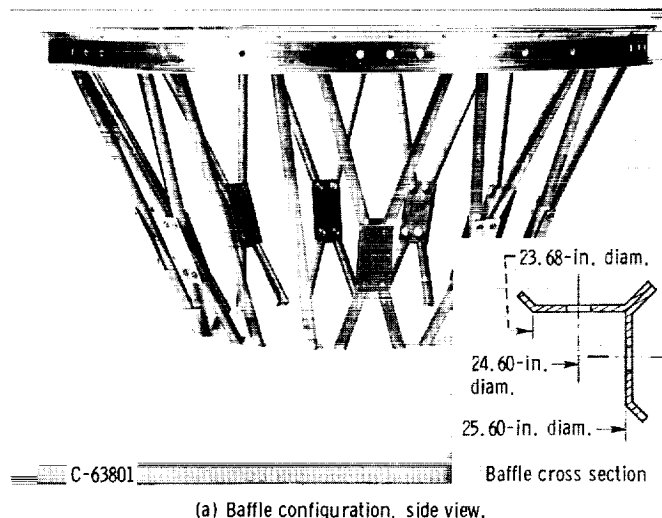


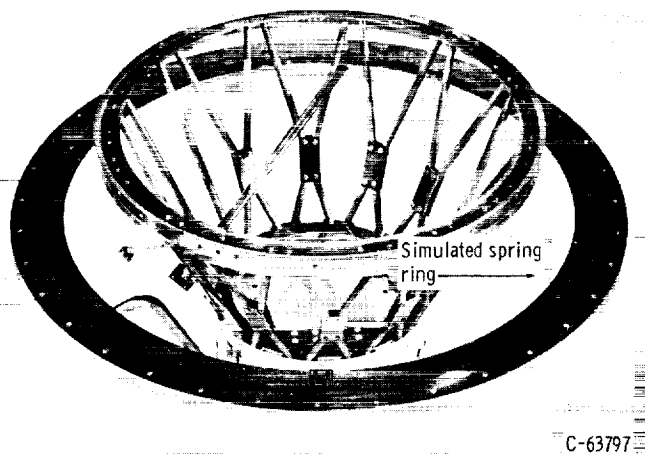
Figure 2 - Scale-model propellant tank.

oxygen tank was fabricated from clear plastic; the major axis a was 32 inches and the minor axis b was 22.86 inches. A cylindrical section 0.88 inch high was located at the equator to simulate the cylindrical portion of the full-scale tank. A $1/3.75$ scale model of each of the following pieces of internal hardware was also constructed (of aluminum): (1) a flat-plate annular-ring baffle 0.73 inch wide, which simulated the spring ring, (2) the thrust distribution cylinder (or thrust barrel), (3) the vent and fill pipes, and (4) the proposed slosh baffle and supporting structure. The clean, unbaffled, and baffled tank configurations shown in figures 2 and 3, respectively, are summarized in the following table:

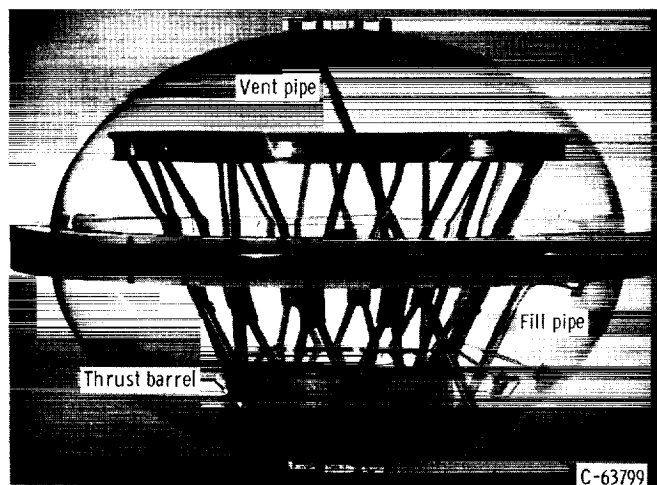
Tank configuration	Internal hardware
Clean (fig. 2(a))	None
Unbaffled (fig. 2(b))	Spring ring, thrust barrel, vent and fill pipes
Baffled (fig. 3)	Spring ring, thrust barrel, vent and fill pipes, slosh baffle and supporting structure



(a) Baffle configuration, side view.



(b) Baffle installation, oblique view.



(c) Baffle installation, side view.

Figure 3. - Proposed scale-model slosh baffle and propellant tank, baffled configuration.

With the exception of the method of assembly, the general configuration of the baffle, its supporting structure, thrust barrel, and vent and fill pipes was identical to their full-scale counterparts. The top and the bottom of the slosh baffle were located at depth ratios $h_b/(b+c)$ of 0.765 and 0.705, respectively. (All symbols are defined in appendix A.) A minimum distance of approximately 0.5 inch was maintained between the edge of the slosh baffle and the tank wall. The contained liquid was water.

PROCEDURE AND DATA REDUCTION

Slosh Force Suppression

Characteristics

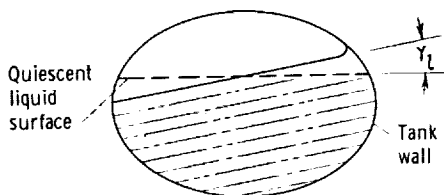
The tank was oscillated sinusoidally at a preselected excitation frequency (0.5 to 2.0 cps) and amplitude (0.100 in.). At each liquid depth ratio investigated, the excitation frequency chosen was equal to the fundamental frequency of oscillation of the contained liquid since this provided the maximum slosh forces at a given excitation amplitude (refs. 6 and 10). These maximum slosh forces are hereinafter referred to as the first mode slosh forces. The excitation amplitude of 0.100 inch was chosen because it was sufficient to provide large slosh forces that could be accurately measured at lower liquid depth ratios and still not create extremely violent liquid oscillations at higher liquid depth ratios. When the first mode waveform had built up to its maximum height on the tank wall, the oscillatory motion of the tank was quick-stopped, and the residual horizontal slosh forces

were recorded on an oscillograph trace.

The fundamental frequencies of the liquid oscillation were determined by using the first several slosh force peaks occurring immediately after the quick stop and were put into the form of the fundamental frequency parameter $\eta = \omega\sqrt{r/g}$. The values of the horizontal slosh forces were determined by using the first force peak occurring immediately after the quick stop; the horizontal force was put into the form of the slosh force parameter, $\lambda = F_s/\rho g a^2(b+c)$. The damping ratios were calculated by averaging the first two successive values of the logarithmic decrement $\delta = \ln(F_{s,n}/F_{s,n+1})$ on each oscillograph trace, where $F_{s,n}$ was the peak force on one slosh cycle and $F_{s,n+1}$ was the peak force on the succeeding cycle.

Quantities for Pendulum Analogy

Slosh angle. - The angle from the horizontal at which the liquid surface oscillated (shown in the sketch at the left) was measured visually by a protractor-type device when the liquid surface had attained its maximum height on the tank wall; the accuracy of this device was about $\pm 1^\circ$.



Hinge point location. - It was desirable to keep the wave height of the liquid oscillation small so that any dependence of the hinge point location on excitation amplitude could be detected at higher liquid depth ratios. Excitation amplitudes of 0.010, 0.020, and 0.030 inch were used; the excitation frequency was equal to the fundamental frequency of the contained liquid. The vertical and horizontal slosh forces were determined by using the first force peaks that occurred immediately after the quick stop; then the external moment M on the tank was calculated. The method of calculating the hinge point location is presented in appendix B.

Pendulum mass. - To obtain the quantities needed in calculating the pendulum mass (or effective sloshing mass) from equation (B7) (see appendix B), it was necessary to determine the horizontal slosh forces for steady-state conditions where the excitation frequency (1) was much less than the fundamental frequency of the contained liquid and (2) was exactly equal to the liquid oscillatory frequency. Excitation frequencies were varied from 40 to 75 percent of the fundamental frequency to determine the effect of a variation of excitation frequency on the values obtained for the pendulum mass. The tank was oscillated at excitation amplitudes of 0.600 and 0.900 inch (1) to drive the wave height of the liquid surface as high as possible, thereby maximizing the slosh forces and their accuracy of measurement, (2) to determine the effect of excitation amplitude on the values obtained for the pendulum mass, and (3) to stay within the operating limits of the test facility. Once the wave height had reached a steady-state value, the oscillatory motion of the tank was quick-stopped, and the horizontal slosh forces were determined from the first force peak occurring immediately thereafter.

EXPERIMENTAL SLOSH FORCE SUPPRESSION CHARACTERISTICS

Fundamental Frequency

The fundamental frequencies of oscillation of the liquid contained in an oblate spheroidal tank may be calculated from the following equation (ref. 12):

$$\Omega = \sigma \sqrt{\frac{g}{r} \epsilon \tanh\left(\frac{h_c}{r} \epsilon\right)} \quad (1)$$

where $h_c = 1/3[h(1.5b - h)/(b - h)]$. The experimental results presented in reference 12 indicate that the correction factor σ was necessary in the calculation of the fundamental frequencies to provide closer agreement between calculated and experimental values over a wide range of liquid depth ratios. The values of σ , which represented a faired curve through the results shown in reference 12 and which were used in this investigation, are presented in figure 4.

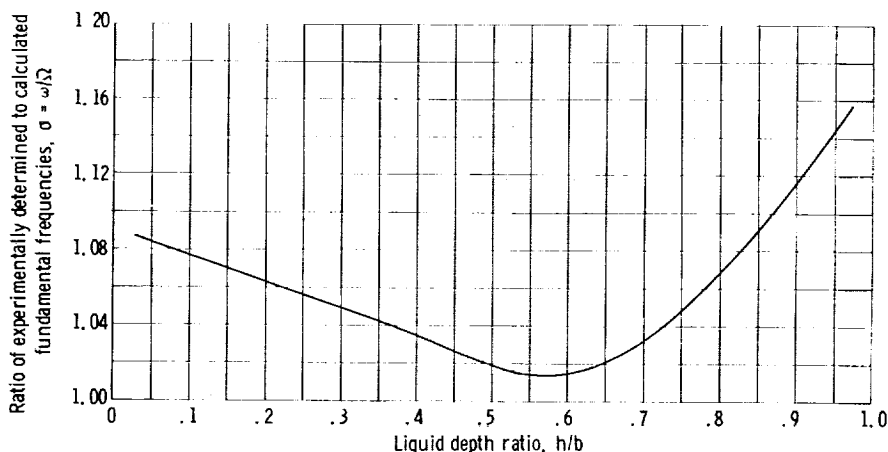


Figure 4. - Ratio of experimentally determined to calculated fundamental frequencies as a function of liquid depth ratio for oblate spheroidal tank (ref. 12).

The values of the fundamental frequency parameter for the clean configuration of the scale-model Centaur liquid oxygen tank were calculated from

$\eta = \sigma \sqrt{\epsilon \tanh\left(\frac{h_c}{r} \epsilon\right)}$. Since the height of the cylindrical section of the tank was small, it was assumed that the fundamental frequency parameter would remain essentially constant for liquid depth ratios in this section. The experimental fundamental frequency parameter $\eta = \omega\sqrt{r/g}$ is compared with the calculated values over a range of liquid depth ratios $0.05 \leq h/(b + c) \leq 0.95$ in figure 5(a). Each data point shown represents an average of several values; the maximum deviation from the average was ± 0.5 percent.

The presence of the thrust barrel in the un baffled tank configuration had a pronounced effect on the fundamental frequency parameter as shown in figure 5(b). When the liquid surface was below the top of the thrust barrel $h/(b + c) < 0.232$, the liquid was contained in essentially two different tanks:

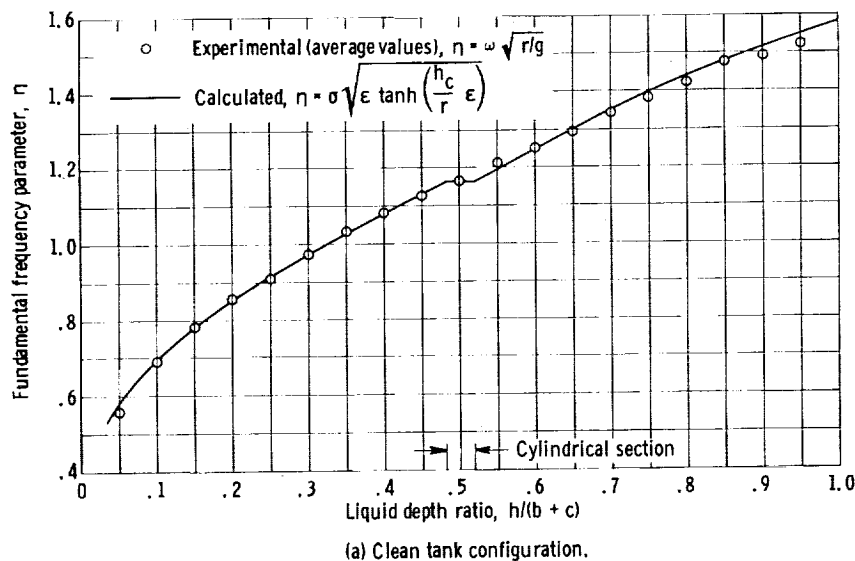
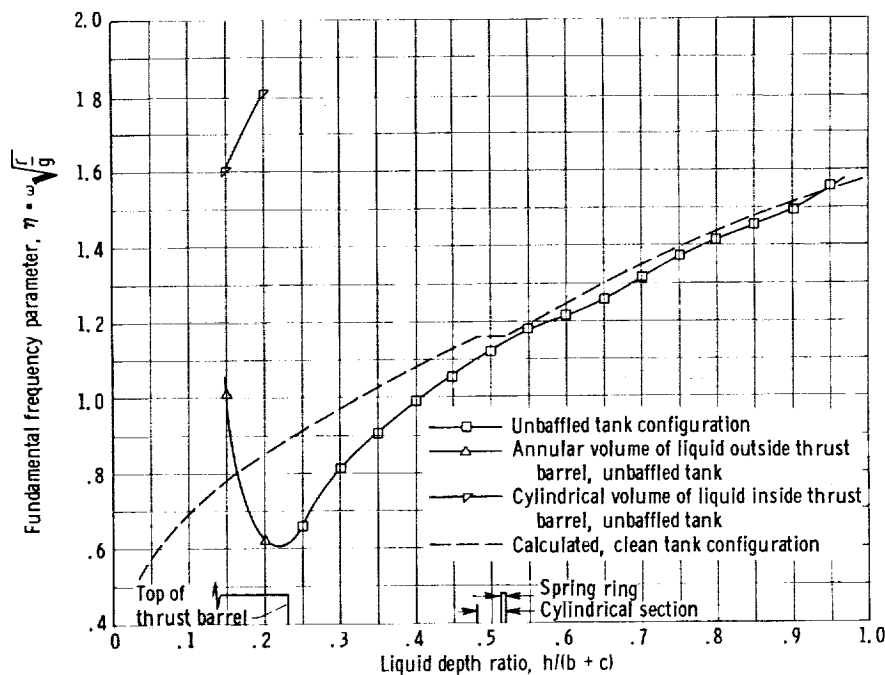


Figure 5. - Fundamental frequency parameter of scale-model propellant tank for varying liquid depth ratio. Excitation amplitude parameter, 0.00313.

the thrust barrel $h/(b+c) > 0.232$, all of the liquid within the tank oscillated as one mass, and the fundamental frequency parameter increased with an increase of the liquid depth ratio. The thrust barrel reduced the fundamental frequency parameter below that obtained in the clean tank configuration up to a liquid depth ratio of 0.50, above which



(b) Unbaffled tank configuration; effect of thrust barrel and spring ring.

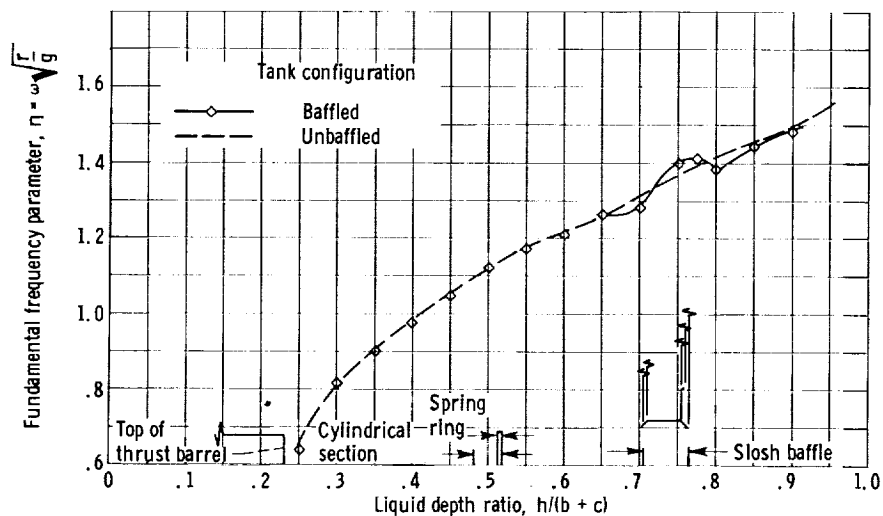
Figure 5. - Continued. Fundamental frequency parameter of scale-model propellant tank for varying liquid depth ratio. Excitation amplitude parameter, 0.00313.

(1) a cylindrical tank formed within the thrust barrel, and (2) an annular tank formed between the thrust barrel and the wall of the oblate spheroidal tank. The cylindrical volume of liquid had higher fundamental frequencies, which tended to increase as the liquid depth ratio increased. The annular volume of liquid had lower fundamental frequencies, which tended to decrease as the liquid depth ratio increased. It was observed that once the liquid surface was above the top of

the thrust barrel $h/(b+c) > 0.232$, all of the liquid within the tank oscillated as one mass, and the fundamental frequency parameter increased with an increase of the liquid depth ratio. The thrust barrel reduced the fundamental frequency parameter below that obtained in the clean tank configuration up to a liquid depth ratio of 0.50, above which value little difference was noted in the fundamental frequency parameter of these two configurations. Each data point (fig. 5(b)) represents an average of several values; the maximum deviation from the average was ± 0.5 percent.

The presence of the slosh baffle in the baffled tank configuration produced only a small variation of the fundamental frequency parameter (liquid depth ratios $0.65 < h/(b+c) < 0.90$) from those values obtained for the unbaffled tank configura-

tion (fig. 5(c)). Each data point again represents an average of several val-



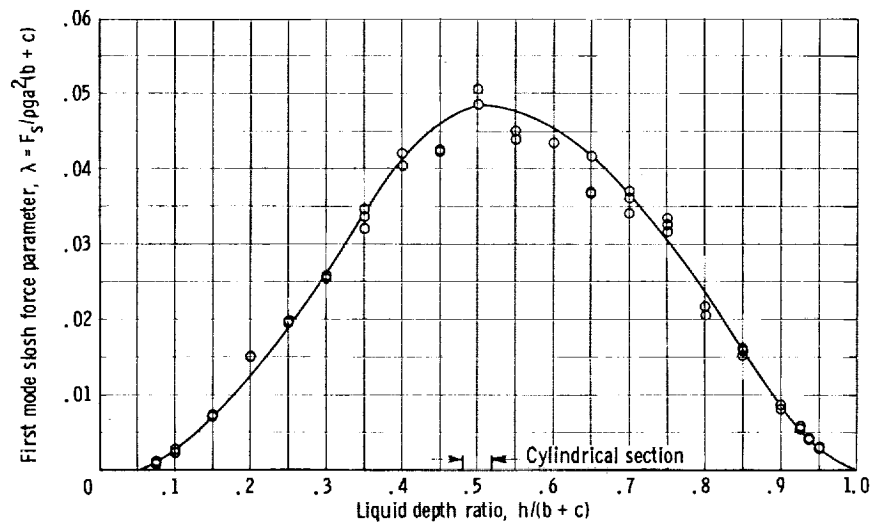
(c) Baffled tank configuration; effect of proposed slosh baffle.

Figure 5. - Concluded. Fundamental frequency parameter of scale-model propellant tank for varying liquid depth ratio. Excitation amplitude parameter, 0.00313.

ues; the maximum deviation from the average was ± 2.0 percent.

Slosh Force Parameter

The first mode slosh force parameters obtained in the clean tank configuration over a range of liquid depth ratios $0.075 \leq h/(b+c) \leq 0.95$ are presented in figure 6(a) for an excitation amplitude parameter $X_0/a = 0.00313$.

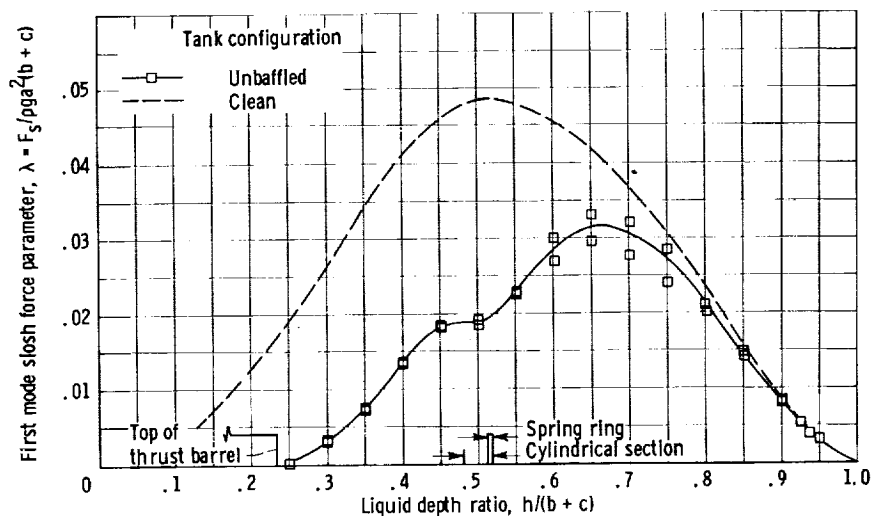


(a) Clean tank configuration.

Figure 6. - First mode slosh force parameter as function of liquid depth ratio. Excitation amplitude parameter, 0.00313.

The maximum slosh force parameter of approximately 0.05 was obtained at a liquid depth ratio of 0.50, and the faired curve was nearly symmetrical about that depth ratio.

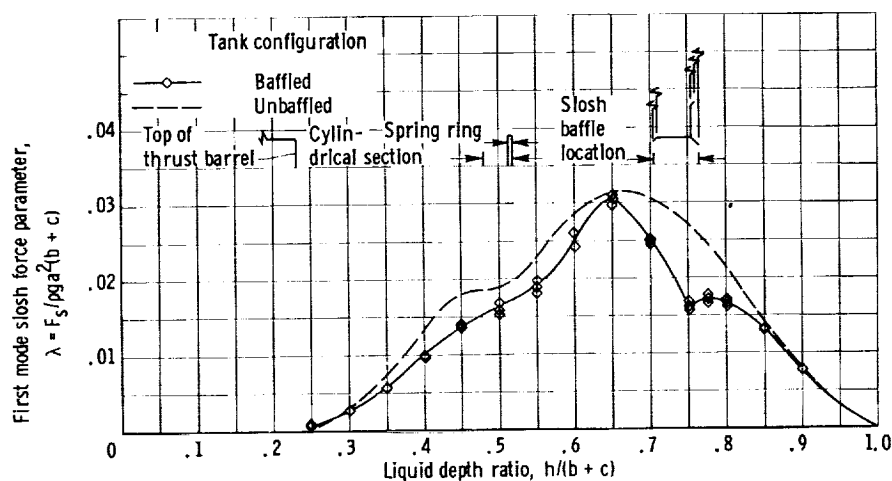
The presence of the thrust barrel and the spring ring in the unbaffled tank configuration resulted in large reductions of the first mode slosh force parameters up to a liquid depth ratio of approximately 0.65 where a maximum force parameter of about 0.03 occurred, as shown in figure 6(b). Little dif-



(b) Unbaffled tank configuration; effect of thrust barrel and spring ring.

Figure 6. - Continued. First mode slosh force parameter as function of liquid depth ratio. Excitation amplitude parameter, 0.00313.

ference in the force parameters obtained in the clean and the unbaffled tank configurations was noted for liquid depth ratios greater than 0.80.



(c) Baffled tank configuration; effect of proposed slosh baffle.

Figure 6. - Concluded. First mode slosh force parameter as function of liquid depth ratio. Excitation amplitude parameter, 0.00313.

The first mode slosh force parameters obtained in the baffled tank configuration are presented in figure 6(c) for a range of liquid depth ratios $0.25 \leq h/(b+c) \leq 0.90$. A maximum slosh force parameter of approximately 0.03 again occurred at a liquid depth ratio of 0.65. However, the supporting structure of the baffle had reduced the slosh force parameters for the range of depth ratios $0.30 < h/(b+c) < 0.65$, and the baffle had reduced the slosh force parameters for depth ratios $0.65 < h/(b+c) < 0.85$. At a liquid depth ratio of 0.80 (an approximate tanking level of the Centaur vehicle) the baffle provided a reduction in slosh force parameter (from ~ 0.021 to ~ 0.017) of about 19 percent.

Damping Ratio

The first mode damping ratios obtained in the clean tank configuration over a range of liquid depth ratios $0.075 \leq h/(b+c) \leq 0.95$ are presented in figure 7(a) for an excitation amplitude parameter $X_0/a = 0.00313$. The increase in damping ratio at the lower depth ratios $0.075 \leq h/(b+c) < 0.15$ is

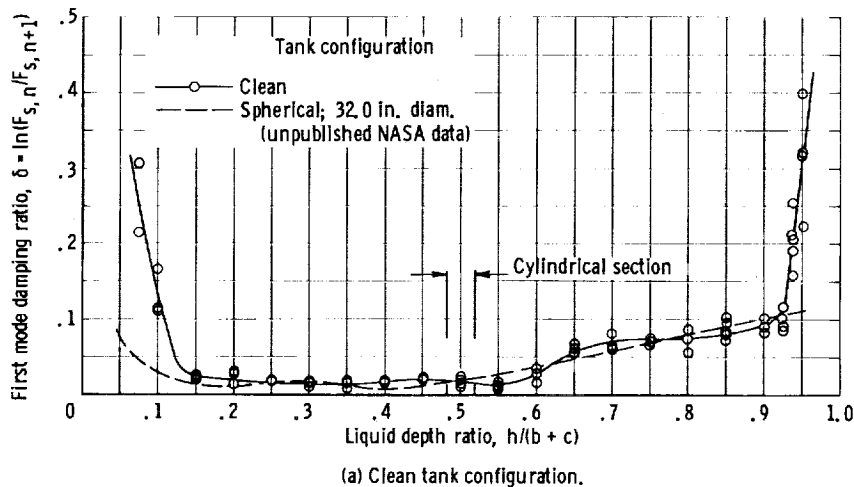
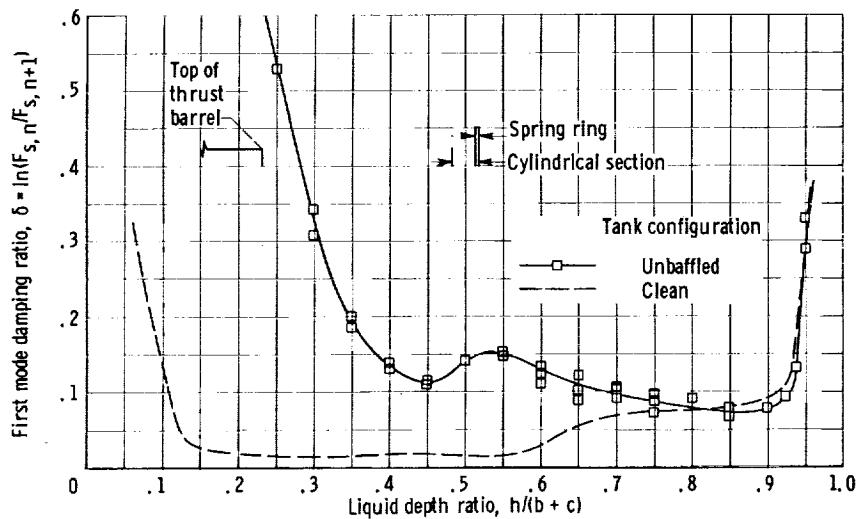


Figure 7. - First mode damping ratio as function of liquid depth ratio. Excitation amplitude parameter, 0.00313.

due to the small liquid mass present oscillating over a comparatively large tank wall area (ref. 8). The increase in damping ratio for depth ratios greater than 0.60 is due to (1) the curvature of the tank wall and (2) the small portion of liquid that splashed from the tank wall, both of which tend to produce ripples on the surface of the liquid. Comparison of these results with those obtained for a spherical tank configuration (unpublished NASA data) indicates that the oblate spheroidal tank provided higher damping ratios for a nearly full or nearly empty tank, but that the damping ratios were of about the same values for both tanks for intermediate liquid depth ratios.

The presence of the thrust barrel and the spring ring in the unbaffled tank configuration resulted in large increases in the first mode damping ratio up to a liquid depth ratio of about 0.70, as shown in figure 7(b). Little



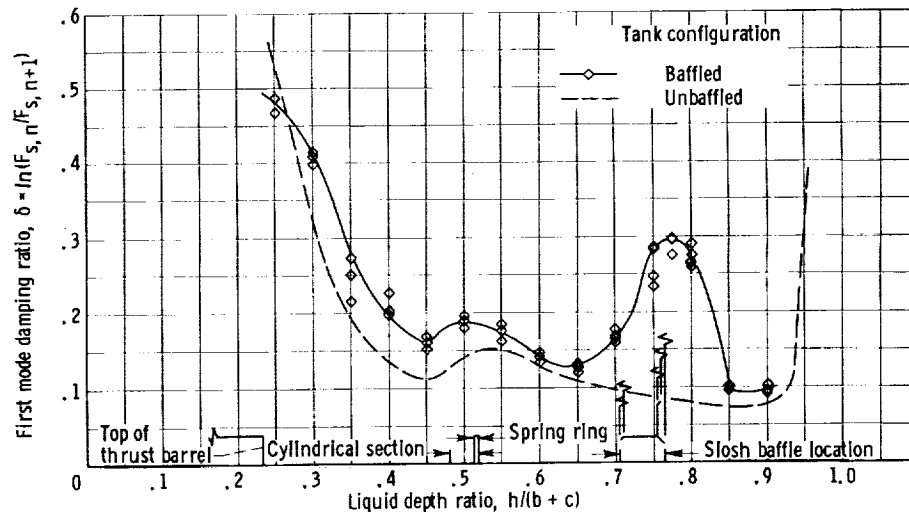
(b) Unbauffed tank configuration; effect of thrust barrel and spring ring.

Figure 7. - Continued. First mode damping ratio as function of liquid depth ratio. Excitation amplitude parameter, 0.00313.

tank configuration over a range of depth ratios $0.25 < h/(b+c) < 0.65$. The slosh baffle increased the damping to a maximum value $\delta \approx 0.3$ at a depth ratio of 0.775. At the depth ratio of 0.80, the damping ratio had been increased from ~ 0.08 to ~ 0.28 .

Scaling Parameters

The values of the fundamental frequencies and the first mode slosh forces that are expected to occur in the full-scale Centaur liquid oxygen tank can be



(c) Baffled tank configuration; effect of proposed slosh baffle.

Figure 7. - Concluded. First mode damping ratio as function of liquid depth ratio. Excitation amplitude parameter, 0.00313.

calculated directly from the fundamental frequency and the slosh force parameters for the tank configurations presented. These slosh forces are the forces that would be produced if the full-scale tank were oscillated at an amplitude of 3/8 inch ($X_0/a = 0.00313$). The values of the slosh force parameters are dependent upon the value of the viscosity parameter of the contained liquid. Reference 10 indicates, however, that the variation of the first mode slosh force parameters obtained in the subscale tank with water and the full-scale tank with liquid oxygen for an excitation amplitude parameter of 0.00313 should be small (less than 5 percent).

It is somewhat more difficult, however, to predict the first mode damping ratios that would be expected to occur in the full-scale Centaur liquid oxygen tank. A liquid depth ratio of 0.80 is of particular interest for the full-scale tank because this is the approximate initial tanking level at which the simulated vehicle instability problems occurred. The damping that occurred at a liquid depth ratio of 0.80 in the clean tank configuration (fig. 7(a)) and the unbaffled tank configuration (fig. 7(b)) is due in part to viscous damping effects at the tank wall. It has been shown in small-scale tests that, for a spherical tank configuration at a liquid depth ratio of 0.50, the first mode damping ratio that resulted from viscous damping could be generalized for tank size and liquid kinematic viscosity when correlated with a viscosity parameter $B = \nu/\sqrt{gd^3}$ where D is the tank diameter (ref. 10). A small amount of data was obtained in the scale-model Centaur liquid oxygen tank with glycerine as the contained liquid ($\nu = 0.01453$ sq ft/sec) at a depth ratio of 0.80 in an attempt to predict damping ratios in the full-scale Centaur liquid oxygen tank in the same manner as for a spherical tank. The results for both the spherical and scale model Centaur liquid oxygen tanks are shown in figure 8. Extrapolation

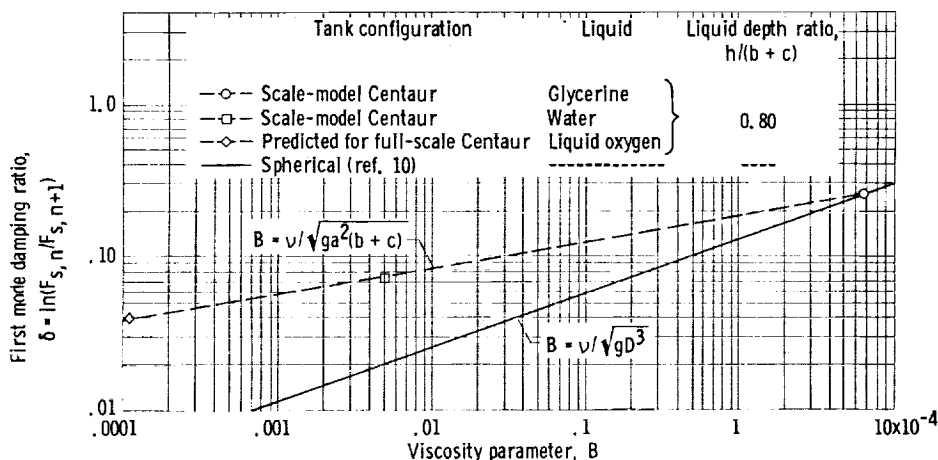


Figure 8. - Effect of viscosity parameter on first mode damping ratio.

tion of these data indicates that at a liquid depth ratio of 0.80, a first mode damping ratio of approximately 0.04 would be expected in the full-scale Centaur tank containing liquid oxygen.

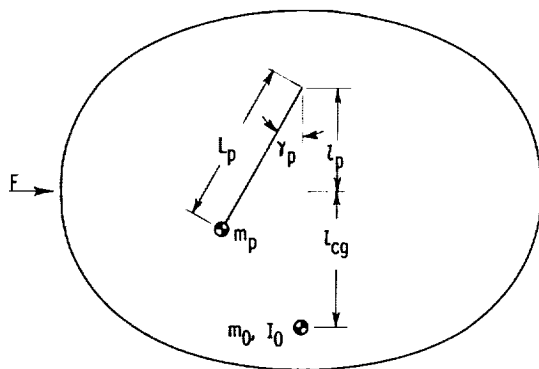
At liquid depth ratios $0.45 < h/(b+c) < 0.60$ in the unbaffled and the baffled tank configurations and $0.65 < h/(b+c) < 0.85$ in the baffled tank

configuration, the damping of the first mode slosh forces was caused by the presence of an annular ring baffle. The values of the damping ratios obtained at these liquid depth ratios in the scale-model Centaur liquid oxygen tank are approximately the values that may be applied directly to tanks of any size having the same configuration provided that the baffle width ratio W/a and the excitation amplitude parameter X_0/a are held constant (ref. 9 and unpublished NASA data for spherical tanks containing annular ring baffles). The first mode damping ratios are also dependent upon the absolute viscosity of the contained liquid. Since the variation between the values of absolute viscosity of water and liquid oxygen is small, however, the damping ratios obtained when water is used can be considered to be close to the values expected for liquid oxygen.

EXPERIMENTAL PENDULUM ANALOGY

The analytical solutions for prediction of the fundamental frequencies and slosh forces in tanks of varying configurations have been solved and proved experimentally (e.g., ref. 6). The use of these solutions in a vehicle dynamic-stability analysis is rather limited, however, because of the complexity of these equations. Therefore, it is highly desirable to obtain suitable linear approximations to represent the propellant sloshing. Two mechanical analogies that have been used to simulate propellant sloshing in vehicle dynamic-stability studies with a great deal of success are the pendulum system and the spring-mass system. The quantities necessary to represent liquid sloshing

characteristics as a pendulum-analogy system (fig. 9) are presented here for the un baffled tank configuration; derivation of the necessary equations and reference to the use of a spring-mass system to represent propellant sloshing is given in appendix B.



Length of Pendulum Arm

The length of the pendulum arm L_p may be calculated directly from the pendulum fundamental frequency expression $L_p = g/\omega^2$. A dimensionless pendulum arm length to tank height ratio $L_p/(b+c)$ is presented in figure 10 for a range of liquid depth ratios $0.25 \leq h/(b+c) \leq 0.95$. The ratio $L_p/(b+c)$ increased as the liquid depth ratio decreased. The pendulum arm length effectively became greater than the tank height at liquid depth ratios $h/(b+c) < 0.285$ because the thrust barrel had reduced the fundamental frequencies to values that were lower than

F	force restraining horizontal motion of tank in test facility, equal to slosh force
I_0	moment of inertia of fixed mass
L_p	length of pendulum arm
l_{cg}	distance from center of tank to centroid fixed mass
l_p	distance from center of tank to pendulum hinge point
m_p	pendulum mass
m_0	fixed mass
γ_p	half-angle from vertical through which pendulum mass oscillates

Figure 9. - Quantities used to describe pendulum analogy of liquid sloshing.

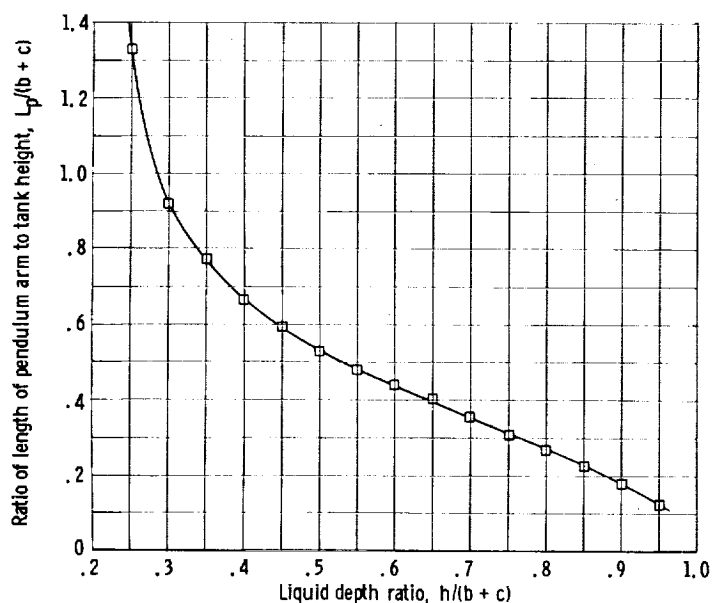


Figure 10. - Ratio of length of pendulum arm to tank height as function of liquid depth ratio for unbaffled tank configuration.

those that occurred in the clean tank configuration (fig. 5(b), p. 8).

Half-Angle of Pendulum

Oscillation

The pendulum arm was assumed to remain normal to the liquid surface at all times (the only logical assumption possible); therefore, the half-angle γ_p through which the pendulum effectively could oscillate was assumed to be equal to the slosh half-angle γ_l . Values of the slosh angle were obtained visually by means of a protractor-type device. The maximum slosh angles through which the liquid

surface could be driven are shown in figure 11. It was observed that the exci-

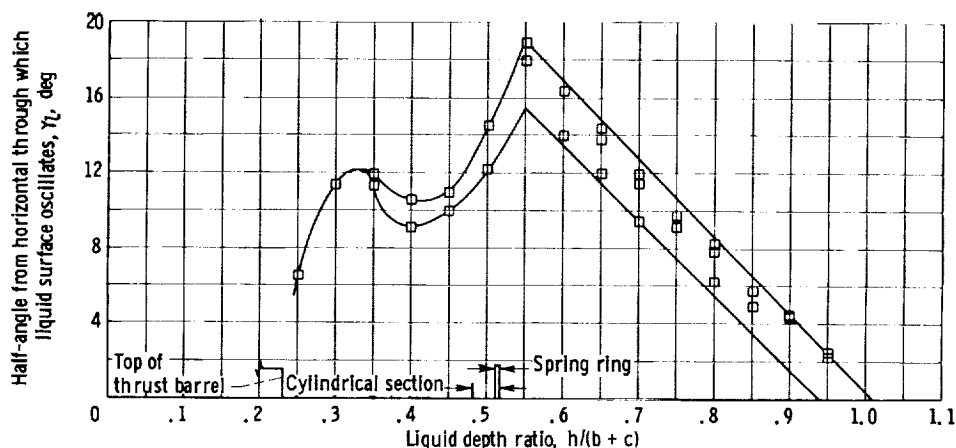


Figure 11. - Maximum angle from horizontal through which liquid surface oscillates as a function of liquid depth ratio for unbaffled tank configuration.

tation amplitudes necessary to drive the liquid to oscillate near the maximum slosh angles were large ($X_0/a > 0.015$) for the lower depth ratios and decreased as the depth ratio increased. At liquid depth ratios $h/(b+c) \geq 0.75$, excitation amplitude parameters $X_0/a \leq 0.000938$ were sufficient to force the liquid to oscillate at its maximum slosh angle.

Location of Hinge Point

The location of the hinge point of the pendulum arm was assumed to lie on

the vertical axis of the tank, and its location on that axis was determined by using the equation $l_p = M/F_g$ (eq. (B9)). A nondimensional ratio of the hinge point location to tank height $l_p/(b + c)$ is presented in figure 12 for excita-

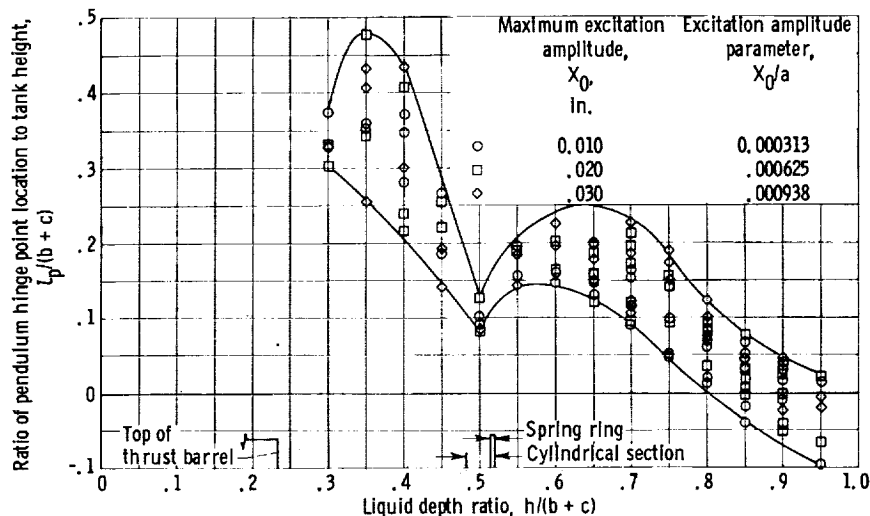


Figure 12. - Ratio of pendulum hinge point location to tank height as function of liquid depth ratio for unbaffled tank configuration.

tion amplitude parameters of 0.000313, 0.000625, and 0.000938. The thrust barrel and the spring ring generally tended to reduce the values of $l_p/(b + c)$ for liquid depth ratios $h/(b + c) < 0.70$. No dependence of the hinge point location on the excitation amplitude parameter was noted. The scatter in the experimental data (fig. 12) resulted because the slosh forces were small and any slight error in measuring either the vertical or horizontal force resulted in a large variation of M . Therefore, figure 12 shows the upper and lower limits between which most of the experimental data appeared rather than a single curve faired through the data.

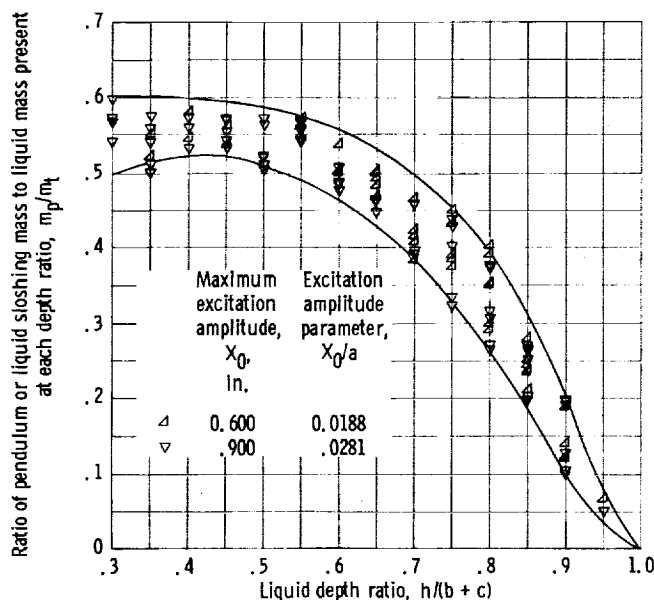


Figure 13. - Ratio of pendulum or liquid sloshing mass to liquid mass present at each depth ratio as function of liquid depth ratio for unbaffled tank configuration.

Pendulum or Sloshing Mass

The effective pendulum mass that would produce oscillatory side forces equal to those that resulted from the sloshing liquid were calculated from equation (B7). The ratio of the experimentally determined sloshing masses to the total

liquid mass present in the tank at the given liquid depth ratio m_p/m_t is presented in figure 13. Values of the ratio m_p/m_t increased as the liquid depth ratio decreased and reached a maximum value ranging from 0.5 to 0.6 at a liquid depth ratio of 0.30. No dependence of the slosh mass ratio on excitation amplitude parameter or excitation frequency was noted. The scatter of the experimental data resulted from the inability to measure the slosh forces with an

accuracy of better than ± 5 percent. Therefore, upper and lower limits encompassing most of the experimental data were drawn on this and remaining figures. The actual values of the slosh mass ratio should lie between these limits.

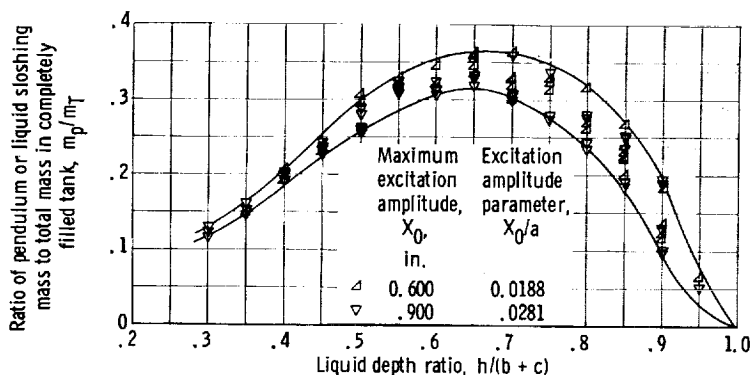


Figure 14. - Ratio of pendulum or liquid sloshing mass to total mass in completely filled tank as function of liquid depth ratio for unbaffled tank configuration.

reached a maximum value (maximum sloshing mass m_p) of 0.315 to 0.365 at a liquid depth ratio of about 0.65 where the maximum slosh forces have also been shown to occur (fig. 6(b), p. 10).

Fixed or Nonsloshing Mass

The fixed mass was determined from equation (B10) (see appendix B). The upper and lower limits of the fixed mass ratio m_0/m_T were determined from the previously shown data (fig. 14) and are presented in figure 15. The fixed mass ratio decreased with a decrease in the liquid depth ratio.

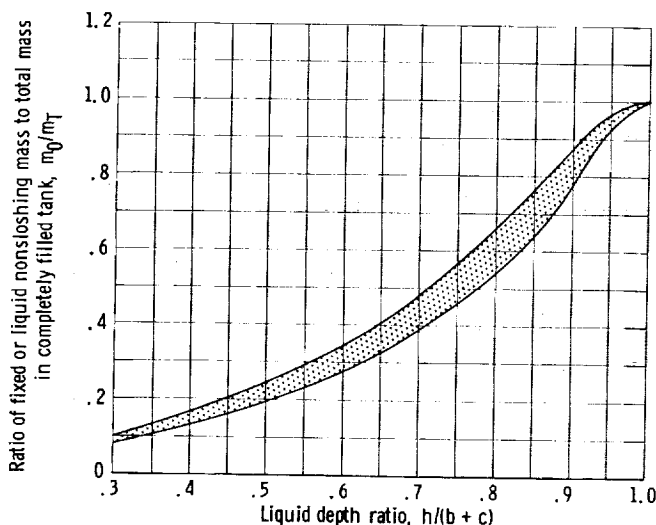


Figure 15. - Ratio of fixed or liquid nonsloshing mass to total mass in completely filled tank as function of liquid depth ratio for unbaffled tank configuration.

Centroid Location of Fixed Mass

The distance l_{cg} from the center of the tank to the geometric centroid of the fixed mass is presented as the dimensionless ratio $l_{cg}/(b+c)$ in figure 16. As expected, the centroid moved toward

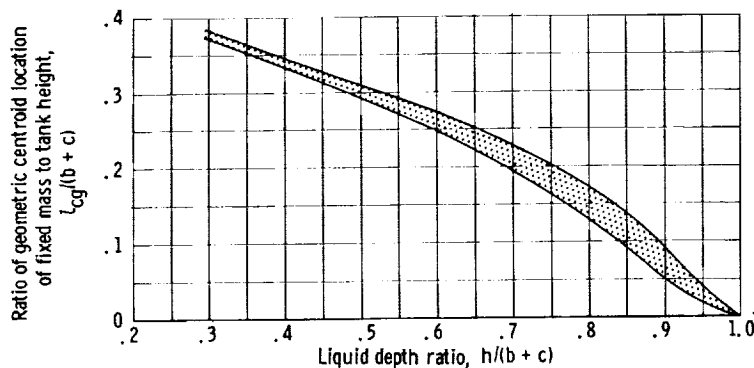


Figure 16. - Ratio of geometric centroid location of fixed mass to tank height as function of liquid depth ratio for unbaffled tank configuration.

the bottom of the tank as the liquid depth ratio decreased.

Scaling Parameters

The values of the dimensionless parameters obtained from this portion of the investigation should be applicable to tanks of any size having the same configuration. (The experimental data should be applied with some degree of caution, however,

since the results of full-scale tests that verify the scaling parameters have not been obtained.)

Since each piece of internal equipment installed within the tank added an unknown quantity in the accuracy and applicability of the experimental results, no attempt was made to experimentally determine a pendulum analogy for the baffled tank configuration. When the dynamic-stability analysis was conducted for this tank configuration, a conservative approach was created by using the pendulum analogy parameters obtained for the unbaffled tank configuration with the values of the damping ratios obtained for the baffled tank configuration.

SUMMARY OF RESULTS

An experimental investigation was conducted for three configurations (clean, unbaffled, and baffled) of a 1/3.75 scale-model Centaur liquid oxygen tank to determine (1) the liquid sloshing characteristics, (2) the slosh damping effectiveness of a proposed slosh baffle, and (3) the quantities that would be necessary to effectively represent the liquid sloshing in the unbaffled tank configuration as a pendulum analogy.

The presence of the thrust barrel reduced the fundamental frequencies of oscillation below those values obtained in the clean tank configuration for liquid depth ratios $0.232 \leq h/(b+c) \leq 0.50$. At liquid depth ratios less than 0.232, the liquid was contained in essentially two different tanks because of the thrust barrel. The spring ring had little or no effect on the fundamental frequencies.

The thrust barrel and spring ring reduced the slosh forces and increased the damping ratios from those values obtained in the clean tank configuration for liquid depth ratios less than 0.80.

The proposed slosh baffle reduced the slosh force parameters only slightly (from 0.021 to 0.017) but increased the damping ratio substantially (from 0.08 to 0.28) at a liquid depth ratio of 0.80 (the approximate tanking level of the full-scale Centaur liquid oxygen tank). The baffle had only a small effect on

the fundamental frequencies of the contained liquid.

The following quantities were determined over a range of liquid depth ratios to effectively describe the liquid sloshing in the unbaffled tank configuration as a pendulum analogy:

1. The length of the pendulum arm increased as the liquid depth ratio decreased.

2. A maximum slosh half-angle or a pendulum half-angle of about 19° was obtained at a depth ratio of 0.55.

3. The distance that the hinge point location of pendulum was located above the center of the tank generally increased with a decrease of depth ratio. The location of this point, however, was also influenced by the thrust barrel and the spring ring.

4. The ratio of the pendulum mass to the liquid mass present at a given depth ratio increased as the depth ratio decreased and attained a maximum value of approximately 0.5 to 0.6 at a depth ratio of 0.30. The ratio of the pendulum mass to the liquid mass present in a completely filled tank increased to a maximum value of 0.315 to 0.365 as the depth ratio decreased to 0.65; the slosh mass ratio then decreased with a further decrease in depth ratio.

5. The fixed mass ratio decreased as the depth ratio decreased.

6. The geometric centroid location of the fixed mass moved downward from the center of the tank as the depth ratio decreased.

The results are presented in terms of dimensionless parameters that are applicable to tanks of any size having similar configurations. The experimental data should be applied with some degree of caution, however, as the results of full-scale tests that verify the scaling parameters have not been obtained.

Lewis Research Center

National Aeronautics and Space Administration
Cleveland, Ohio, April 29, 1964

APPENDIX A

SYMBOLS

a	major spheroidal axis of tank, ft
B	viscosity parameter, $\nu/\sqrt{ga^2(b+c)}$
b	minor spheroidal axis of tank, ft
c	height of cylindrical section of tank, ft
D	spherical tank diameter, ft
F	force on tank producing propellant sloshing, lb
F_s	horizontal slosh force, lb
g	vertical acceleration of tank, 32.174 ft/sec ² for this investigation
h	liquid depth (measured from liquid surface to bottom of tank), ft
$h/(b+c)$	liquid depth ratio
h_b	distance from baffle or some location in tank measured vertically to bottom of tank, ft
h_c	liquid depth in cylindrical tank of radius r containing same liquid volume as that contained in oblate spheroidal tank, ft
I_0	moment of inertia of nonsloshing or fixed mass, slug/sq ft
K_s	spring constant, lb/ft
L_p	length of pendulum arm, ft
l_{cg}	distance from center of tank to geometric centroid of fixed mass, ft
l_p	distance from center of tank to pendulum hinge point, ft
M	external moment on tank produced by liquid sloshing, ft-lb
m_p	pendulum or effective liquid sloshing mass, slugs
m_T	total liquid mass present in completely filled tank, slugs
m_t	total liquid mass present in tank at a given liquid depth ratio, slugs
m_0	fixed or liquid nonsloshing mass, slugs

q	vehicle center of rotation
r	radius of liquid surface of partly filled oblate spheroidal tank, ft
W	baffle width, ft
X_0	maximum excitation amplitude, ft
X_0/a	excitation amplitude parameter
x_0	excitation amplitude of tank at any time t , $X_0 \sin \omega_0 t$, ft
γ_l	half-angle from horizontal through which liquid surface oscillates, radians
γ_p	half-angle from vertical through which pendulum oscillates, radians
δ	damping ratio or logarithmic decrement, $\ln(F_{s,n}/F_{s,n+1})$
ϵ	first root of $J_1'(\epsilon_n) = 0$, 1.841
η	fundamental frequency parameter, $\sigma\sqrt{\epsilon \tanh(h_c/r)\epsilon}$ and $\omega\sqrt{r/g}$
$\ddot{\theta}$	angular acceleration of vehicle about q , radians/sec ²
λ	slosh force parameter, $F_s/\rho g a^2(b + c)$
ν	liquid kinematic viscosity, sq ft/sec
ξ	damping factor, $\delta/2\pi$
ρ	liquid mass density, slugs/cu ft
σ	ratio of experimentally determined to calculated fundamental frequencies of liquid oscillations, ω/Ω
Ω	calculated fundamental (first natural mode) frequency of liquid oscillation, radians/sec
ω	experimentally determined fundamental (first natural mode) frequency of liquid oscillation, radians/sec
ω_0	input excitation frequency of tank, radians/sec

Superscripts:

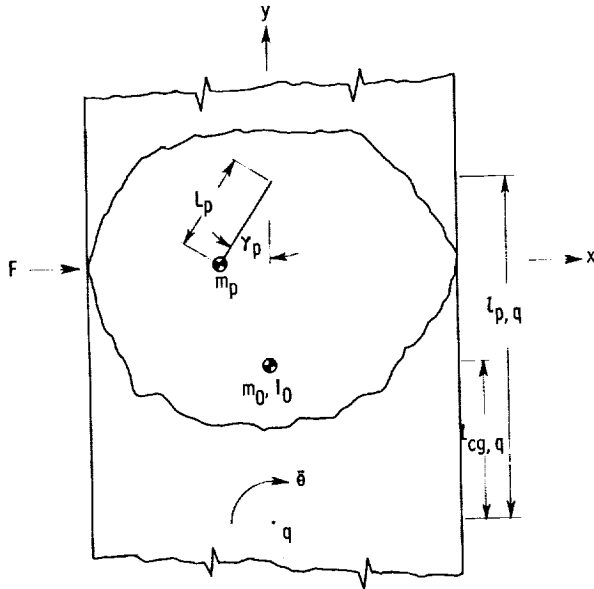
- ($\dot{}$) first time derivative
- ($\ddot{}$) second time derivative

APPENDIX B

PRESENTATION OF LIQUID SLOSHING AS A MECHANICAL ANALOGY

The dynamic-stability analysis of any rigid or flexible liquid fuel space vehicles must include an adequate description of the liquid sloshing that occurs in partly filled propellant tanks. The development of a reliable analytical mechanical model of liquid sloshing for any arbitrary tank configuration is needed. Since a specific tank configuration may be relatively difficult to

analyze mathematically, an accurate experimental technique was needed so that mechanical model parameters could be obtained from simple experimental measurements. The experimental techniques of obtaining the mechanical model parameters presented in this investigation are believed to be adequate for most clean tank configurations; the effect of the presence of internal equipment within the tank on the accuracy of results is not known at the present time.



The sketch at the left shows an arbitrary propellant tank configuration in a rigid body vehicle or test facility. The summation of forces exerted on the tank in the x-direction that result in liquid sloshing may be written as (ref. 5)

$$F = -m_0 \ddot{x}_0 - m_0 l_{cg,q} \ddot{\theta} + m_p g \gamma_p \quad (B1)$$

The summation of forces acting on the pendulum may be written as (ref. 5)

$$m_p L_p \ddot{\gamma}_p + 2m_p \xi \omega L_p \dot{\gamma}_p + m_p L_p \omega^2 \gamma_p = -m_p \ddot{x}_0 - m_p (l_{p,q} - L_p) \ddot{\theta} \quad (B2)$$

where $\xi = \delta/2\pi$. The summation of moments about the vehicle center of rotation q may be written as (ref. 5)

$$M = -m_0 l_{cg,q} \ddot{x}_0 - (I_0 + m_0 l_{cg,q}^2) \ddot{\theta} + m_p l_{p,q} g \gamma_p \quad (B3)$$

Small angle approximations have been assumed in the preceding equations.

In this investigation the tank and test facility were not subjected to any rotational motion so that $\ddot{\theta} = 0$. In addition, the normal test procedure was to oscillate the tank and the contained liquid at a given excitation frequency and amplitude until the liquid surface had attained its maximum wave height.

Once the motion of the tank had been quick-stopped, \ddot{x}_0 was equal to zero, and the forces resulting only from the liquid motion were experimentally measured ($F = F_s$). Equation (B1) may then be written as

$$F_s = m_p g \gamma_p \quad (B4)$$

The pendulum mass may be calculated from equation (B4) once the pendulum angle γ_p corresponding to a specific slosh force F_s is known. The angle γ_p may be measured directly if the pendulum arm is assumed to remain normal to the liquid surface ($\gamma_p = \gamma_l$). This is considered to be a valid assumption. It was difficult to obtain accurate measurements of the liquid slosh angle γ_l visually, however, so a second method of determining the pendulum mass was utilized.

Equation (B2) may be rewritten as

$$m_p L_p (\ddot{\gamma}_p + \omega^2 \gamma_p) = -m_p \ddot{x}_0 \quad (B5)$$

with the following conditions:

- (1) No angular rotation of the test facility ($\ddot{\theta} = 0$)
- (2) The damping term is considered negligible ($2m_p \xi \omega L_p \dot{\gamma}_p \approx 0$)
- (3) The liquid and tank are oscillated sinusoidally

When the liquid was oscillated at an excitation frequency much less than its fundamental frequency ($\omega_0 \ll \omega$), the liquid oscillated at exactly the excitation frequency as long as the oscillatory motion of the tank continued. Since γ_p was assumed to be equal to γ_l , it can also be assumed that $\ddot{\gamma}_p = \ddot{\gamma}_l = -\omega_0^2 \gamma_p \sin \omega_0 t$ or at the maximum wave height of the liquid surface $\ddot{\gamma}_p = \ddot{\gamma}_l = -\omega_0^2 \gamma_p$. By making this substitution, equation (B5) becomes:

$$m_p L_p \gamma_p (-\omega_0^2 + \omega^2) = -m_p \ddot{x}_0 \quad (B6)$$

Equation (B6) must be again rewritten in terms of measurable quantities by making the following substitutions:

- (1) $L_p = g/\omega^2$
- (2) $\ddot{x}_0 = -\omega_0^2 X_0$ (at maximum wave height of liquid surface)
- (3) $m_p = F_s/g\gamma_p$ (substitute into left side only of eq. (B6))

The resulting equation is then

$$m_p = \frac{F_s}{X_0} \left(\frac{1}{\omega_0^2} - \frac{1}{\omega^2} \right) \quad (B7)$$

Equation (B7) is valid for determining the pendulum mass (or effective sloshing mass) as long as the damping factor ξ is small, so that the damping term in equation (B2) may be considered negligible. Therefore, the value of the first force peaks occurring immediately after the quick stop is of almost the same value as the slosh forces that occurred while the tank was subjected to the oscillatory motion.

The hinge point location of the pendulum may be determined by rewriting equation (B3) as the summation of moments about the center of the tank ($\ddot{\theta} = 0$):

$$M = -m_0 l_{cg} \ddot{x}_0 + m_p l_p g \gamma_p \quad (B8)$$

Since $m_p = F_s / g \gamma_p$ and $\ddot{x}_0 = 0$ after the tank has been quick-stopped, the location of the hinge point above the center of the tank may be determined from the equation

$$l_p = M / F_s \quad (B9)$$

No feasible method was available to experimentally determine the fixed mass (or effective nonsloshing mass) and its centroid location. It may be assumed, however, that the fixed mass may be determined from the equation

$$m_0 = m_t - m_p \quad (B10)$$

If it is further assumed that the effective sloshing and nonsloshing masses formed distinct stratified layers in the tank, the location of the centroid of the nonsloshing mass on the vertical axis of the tank may be easily determined by means of geometry.

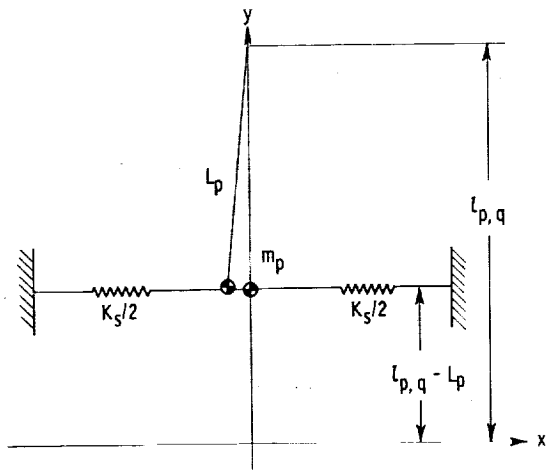
The pendulum analogy may be converted into a spring-mass model in such cases where the latter is more convenient to use. The identical sloshing

forces and moments may be obtained from both models by using equal sloshing masses m_p and by attaching the spring mass at the zero-deflection pendulum mass point as shown in the sketch at the left. The proper spring constant K_s may be obtained from the spring-mass fundamental frequency expansion

$$K_s = m_p \omega^2 \quad (B11)$$

where m_p and ω are the same values used in the pendulum analogy.

The mechanical sloshing models may be used in a dynamic analysis by attaching the models to the vehicle rigid body axis at the proper tank locations. The equations of motion for the entire vehicle



may then be written for the frozen mass vehicle and the sloshing mass vehicle as they respond to steering, aerodynamic, and thrust forces. These equations of motion must be written for a given tanking level since the sloshing model parameters vary with the amount of propellant that remains in each tank.

REFERENCES

1. Bauer, Helmut F.: Propellant Sloshing. Rep. DA-TR-18-58, Army Ballistic Missile Agency, Nov. 5, 1958.
2. Bauer, Helmut F.: Fluid Oscillation in a Cylindrical Tank with Damping. Rep. DA-TR-4-58, Army Ballistic Missile Agency, Apr. 23, 1958.
3. Abramson, H. Norman, and Ransleben, Guido E., Jr.: Simulation of Fuel Sloshing Characteristics in Missile Tanks by Use of Small Models. Tech. Rep. 7, Southwest Res. Inst., Apr. 25, 1960.
4. O'Neill, J. P.: An Experimental Investigation of Sloshing. TR-59-0000-09960, Space Tech. Lab., Inc., Mar. 4, 1960.
5. Lukens, David R., Schmitt, Alfred F., and Broucek, George T.: Approximate Transfer Functions for Flexible-Booster-and-Autopilot Analysis. WADD TR-61-93, General Dynamics Corp., Apr. 1961.
6. Stofan, Andrew J., and Armstead, Alfred L.: Analytical and Experimental Investigation of Forces and Frequencies Resulting from Liquid Sloshing in a Spherical Tank. NASA TN D-1281, 1962.
7. Abramson, H. Norman, Chu, Wen-Hwa, and Garza, R. Luis: Liquid Sloshing in Spherical Tanks. Tech. Rep. 2, Southwest Res. Inst., Mar. 1962.
8. Stephens, David G., Leonard, H. Wayne, and Silveira, Milton A.: An Experimental Investigation of the Damping of Liquid Oscillations in an Oblate Spheroidal Tank With and Without Baffles. NASA TN D-808, 1961.
9. Silveira, Milton A., Stephens, David G., and Leonard, H. Wayne: An Experimental Investigation of the Damping of Liquid Oscillations in Cylindrical Tanks with Various Baffles. NASA TN D-715, 1961.
10. Sumner, Irving E., and Stofan, Andrew J.: An Experimental Investigation of the Viscous Damping of Liquid Sloshing in Spherical Tanks. NASA TN D-1991, 1963.
11. Kendall, G., and Martin, R.: First Mode SLOSH Characteristics of the Centaur LOX Tank. Rep. 55B 1451-1, General Dynamics/Astronautics, May 9, 1962.
12. Leonard, H. Wayne, and Walton, William C., Jr.: An Investigation of the Natural Frequencies and Mode Shapes of Liquids in Oblate Spheroidal Tanks. NASA TN D-904, 1961.